Supporting information

A new approach for the ultra-high loading of curcumin onto a nano-sized ZIF-68 as an effective drug delivery system with good biocompatibility and efficient anti-cancer therapy

Duy Ba Nguyen,[a] Phuong Bich Tran,[a] Quynh Ngoc Thi Luong,[a] Viet Ngoc Huynh,[a] Anh Ngoc Thi Phan,[a] Vu Tuyet Luu,[a] Duong Hoang Dang,[a] Hung Ngoc Nguyen,[a] Loc Cam Luu,[b,d] Tan Le Hoang Doan[c,d] and My Van Nguyen*[a]

[a]Faculty of Chemistry, Ho Chi Minh City University of Education, Ho Chi Minh City, 700000, Vietnam.

[b]HCMC University of Technology, VNU-HCM, 268 Ly Thuong Kiet, District 10, Ho Chi Minh City, Vietnam.

[c]Center for Innovative Materials and Architectures (INOMAR), Ho Chi Minh City, Vietnam.

[d]Vietnam National University, Ho Chi Minh City, Vietnam.

*To whom correspondence should be addressed: mynv@hcmue.edu.vn

Section S1. The Standard Curve of Curcumin

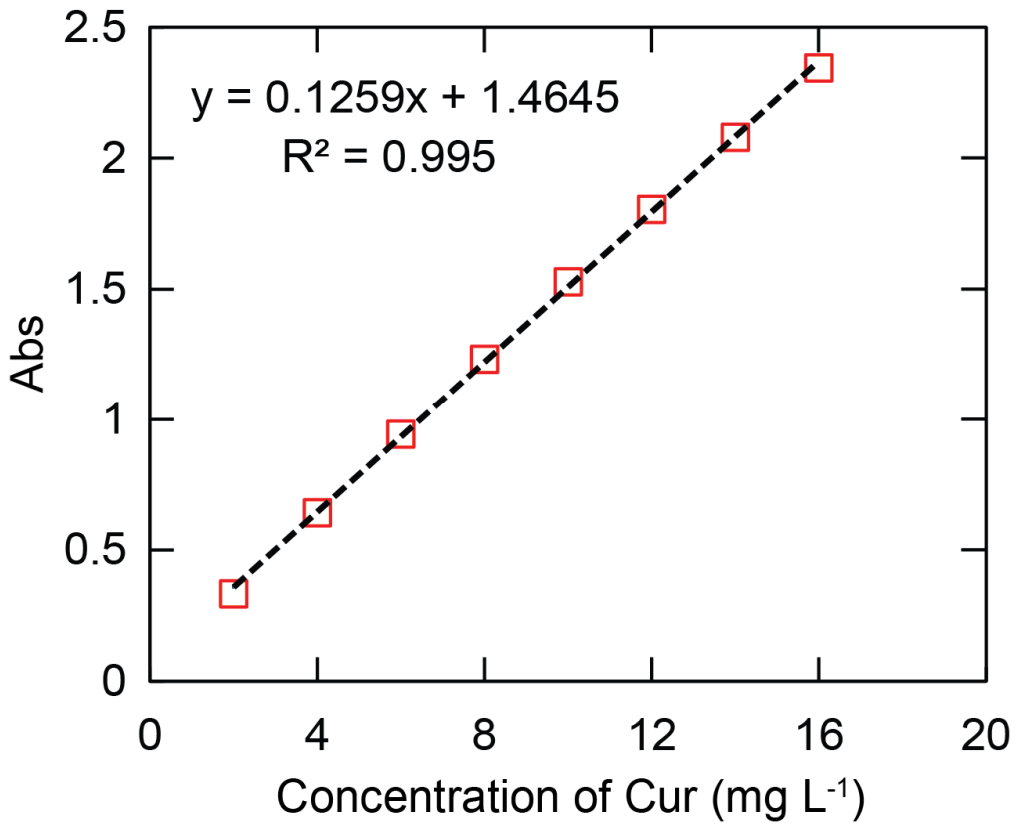

Figure S1. The relationship between the absorbed intensity and the Cur various concentrations of 2 – 20 mg L^{-1} by linear fitting.

Section S2. Elemental Mapping Spectroscopy

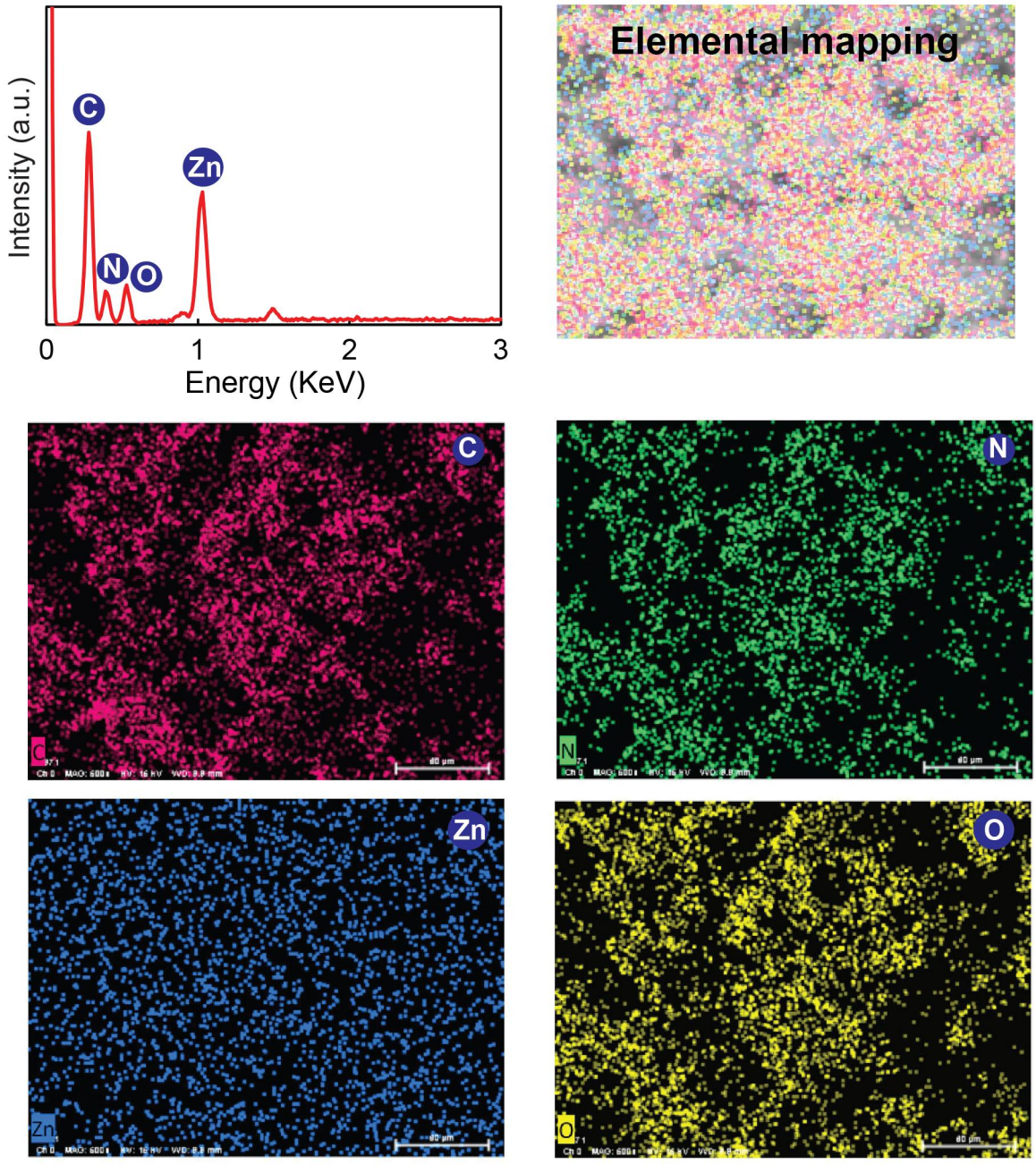

Figure S2. Elemental mapping by SEM-EDX of activated ZIF-68.

Section S3. The Stability of ZIF-68 after Cur Loading

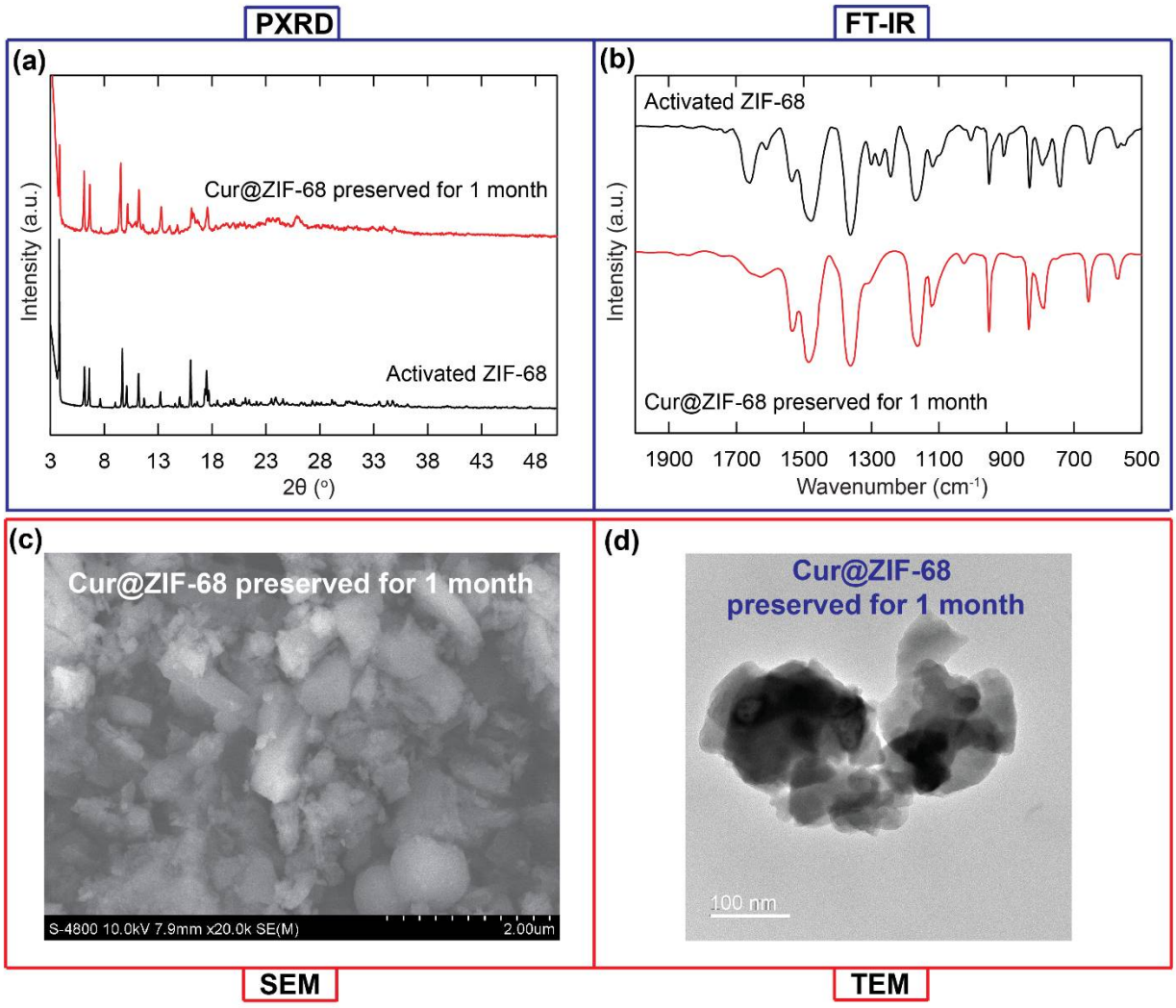

Figure S3. The PXRD pattern of activated ZIF-68 (black) in comparison with the PXRD pattern of Cur@ZIF-68 preserved for 1 month (red) (a); The FT-IR spectra of activated ZIF-68 (black) in comparison with the PXRD pattern of Cur@ZIF-68 preserved for 1 month (red) (b); SEM image at a scale bar of 2μm (c) and TEM image at a scale bar of 100 nm (d) of Cur@ZIF-68 preserved for 1 month.

Section S4. X-ray Photoelectron Spectroscopy

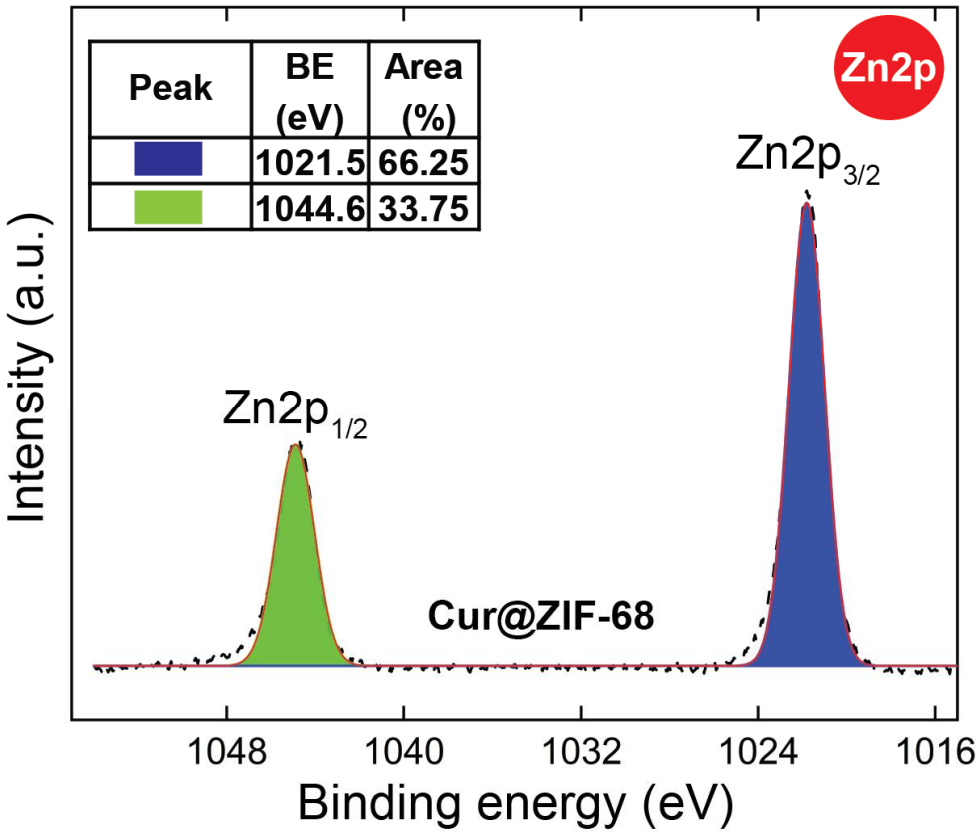

Figure S4. The high-resolution spectrum of Zn 2p in Cur@ZIF-68.

Section S5. In Vitro Drug Release Experiments

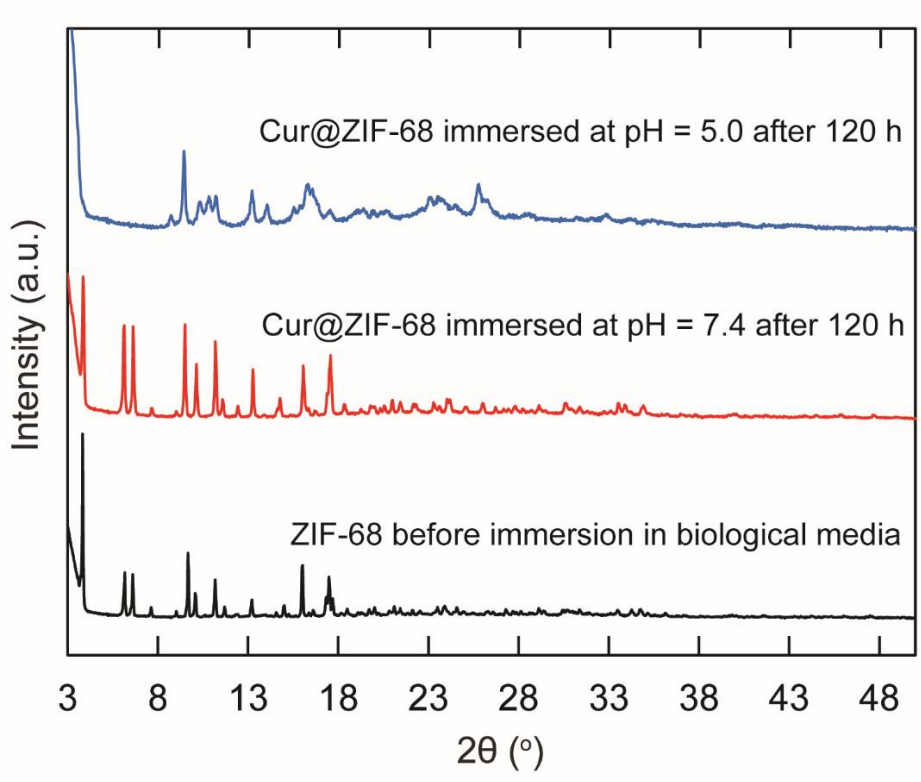

Figure S5. The PXRD pattern of ZIF-68 (black) in comparison with the PXRD patterns of Cur@ZIF-68 immersed at pH = 7.4 (red) and 5.0 (blue) after 120 h

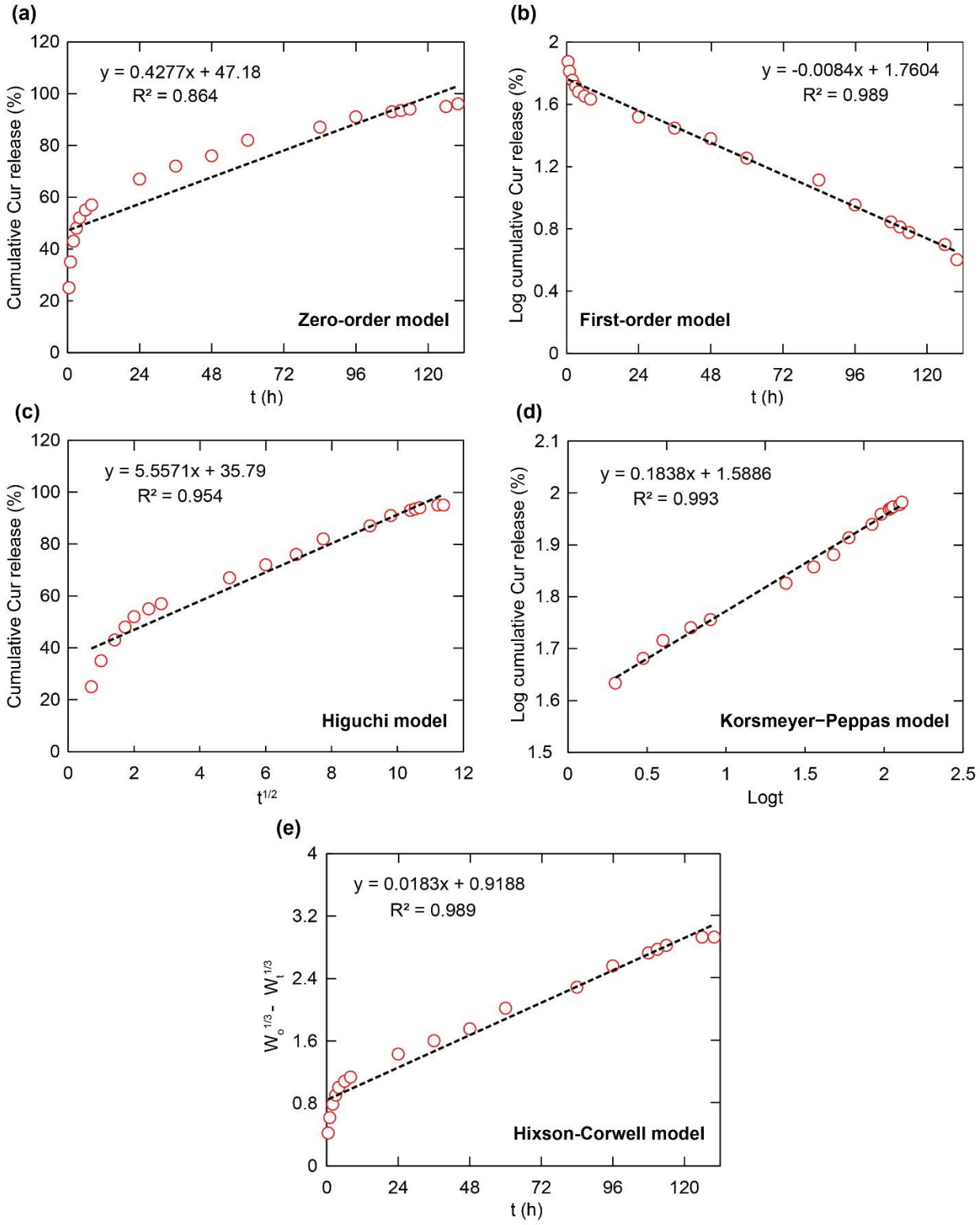

Figure S6. The release profile of Cur@ZIF-68 at pH 5.0

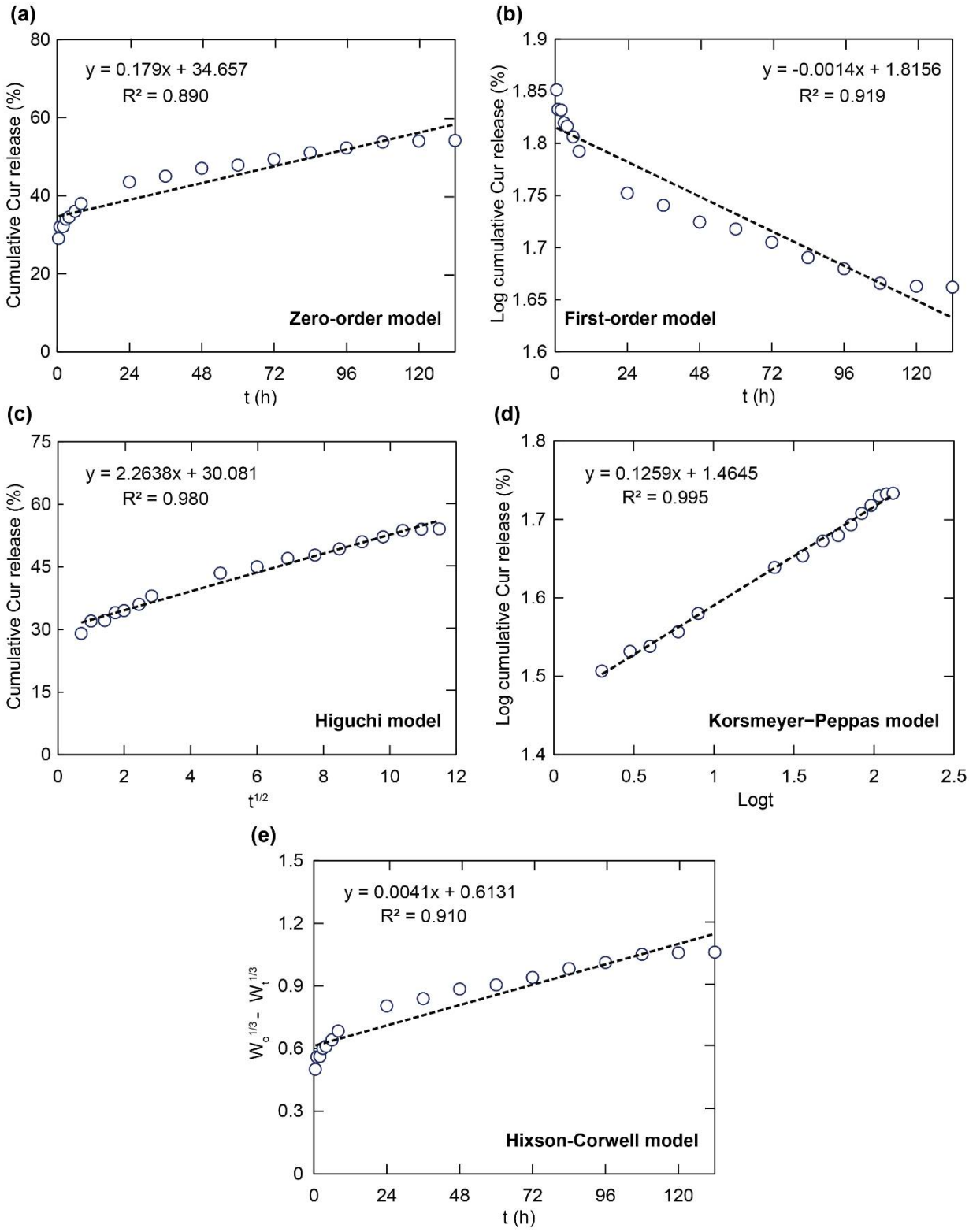

Figure S7. The release profile of Cur@ZIF-68 at pH 7.4

Section S6. Bright-Filed Microscopy Images

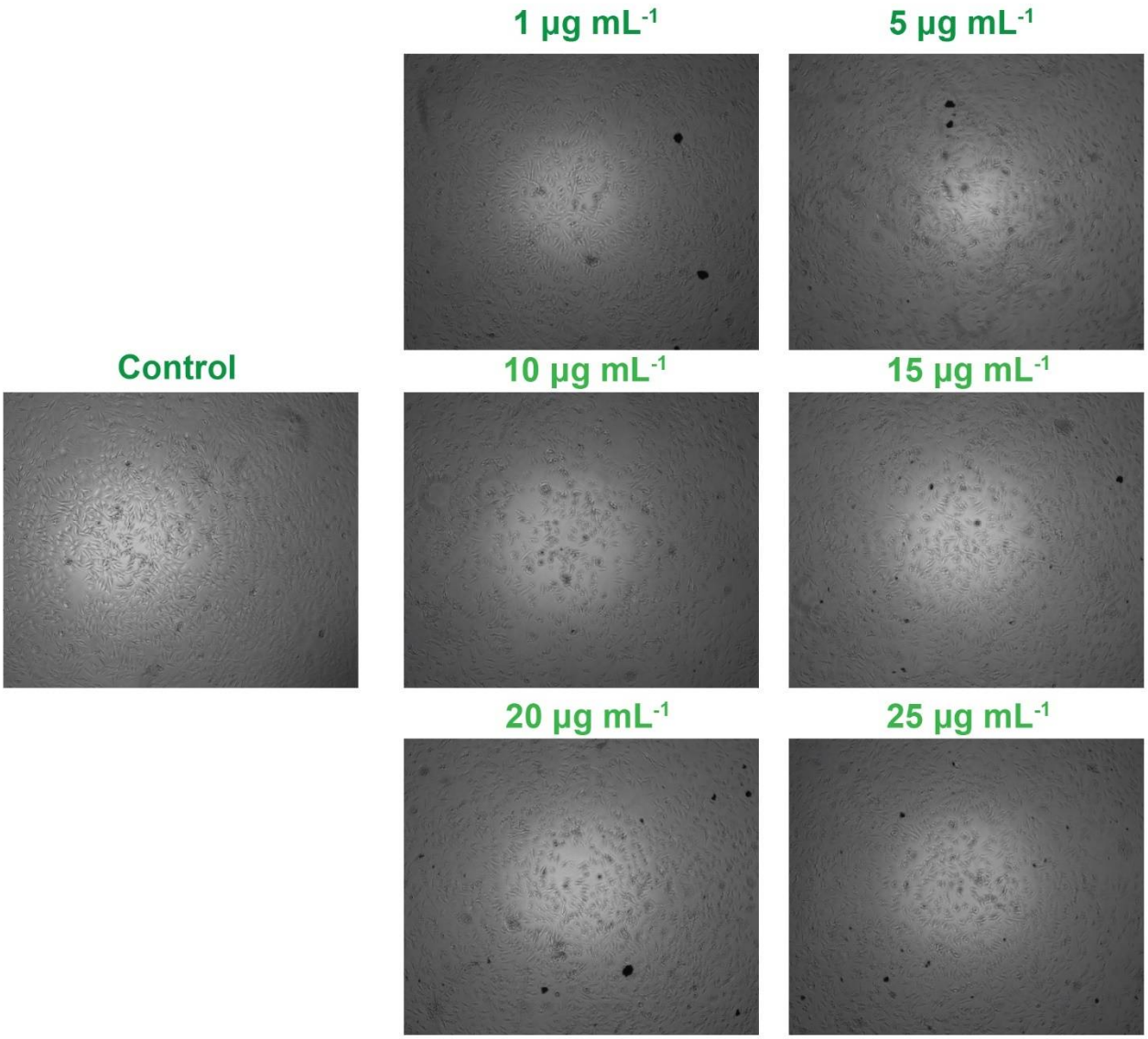

Figure S8. The bright-field microscopy images of ZIF-68 were collected from the cytotoxicity experiment towards the HDF normal cells.

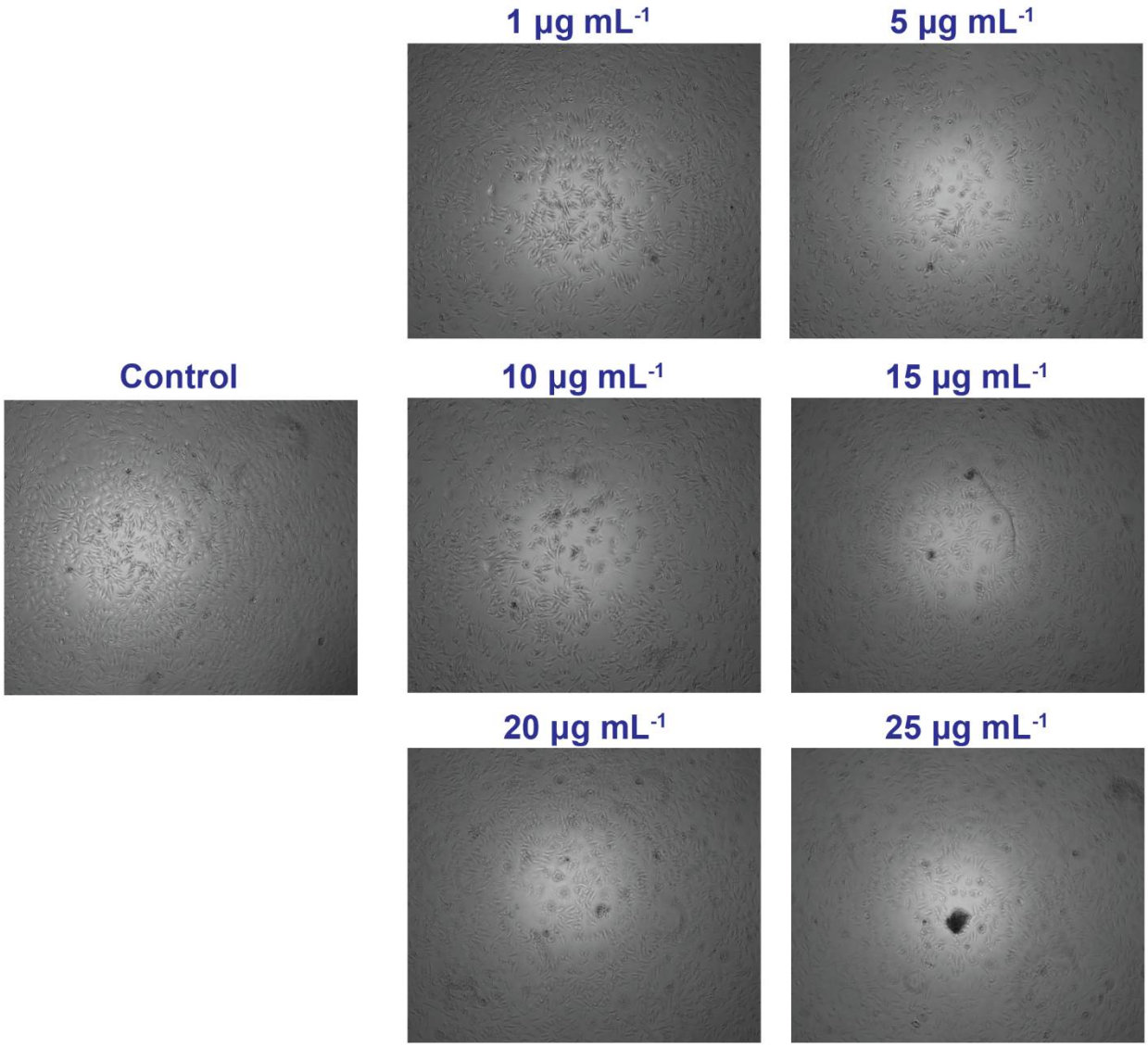

Figure S9. The bright-field microscopy images of Cur@ZIF-68 were collected from the cytotoxicity experiment towards the HDF normal cells

Section S7. The Loading Studies of Cur over ZIF-68

The drug loading content (DLC) and drug loading efficiency (DLE) of ZIF-68 are determined by the following equations:

DLC(%) = (amount of loaded drug)
/(total amount of drug loaded nanoparticles) x 100% (S1)

DLE(%) = (amount of loaded drug)
/(total amount of feeding drug) x 100% (S2)

The linear forms of the Langmuir, Freundlich, Temkin, and Dubinin-Radushkevich (DR) are exhibited by the equations (S3)-(S6):

$$\frac{C_e}{q_e} = \frac{1}{K_L q_m} + \frac{C_e}{q_m} \quad (S3)$$

$$\log q_e = \log K_F + \frac{1}{n}\log C_e \quad (S4)$$

$$q_e = \frac{RT}{b}\ln(k_T C_e) \quad (S5)$$

$$\ln q_e = \ln k_{DR} - C\varepsilon^2 \quad (S6)$$

Where C_e (mg L^{-1}) and q_e (mg g^{-1}) are the Cur concentration and uptake capacity at equilibrium, respectively, q_m (mg g^{-1}) is the theoretical maximum capacity of the Cur loading. K_L (L mg^{-1}) and K_F (mg g^{-1} (L $g^{-1})^{1/n}$) indicate the Langmuir and Freundlich constants, respectively. 1/n parameter represents the uptake index of Freundlich isotherm. *R* is the gas constant, β and k_T are the constant of adsorption heat and the constant of Temkin, respectively, and *T* is the adsorption temperature. Meanwhile, k_{DR} and C are the constants of DR isotherm and the adsorption energy per adsorbent molecule, and ε is a constant.

The separation coefficient of R_L is calculated by equation (S7):

$$R_L = \frac{1}{1 + K_L C_o} \quad (S7)$$

Where C_o and K_L are the initial concentration of Cur and the constant of Langmuir, respectively.

The pseudo-first-order and pseudo-second-order kinetics are used to confirm the uptake rate of Cur onto ZIF-68, which are illustrated by the equations:

$$\ln(q_e - q_t) = \ln q_e - k_f t \quad \text{(S8)}$$

$$\frac{t}{q_t} = \frac{1}{k_s . q_e^2} + \frac{t}{q_e} \quad \text{(S9)}$$

Where q_t and q_e are the Cur adsorption amount at *t* and equilibrium, k_f and k_s are the rate constants of pseudo-first-order and pseudo-second-order models, respectively.

Section S8. The In Vitro Release Testing of Cur@ZIF-68

The linear forms of the kinetic models such as zero-order, first-order, Higuchi, Korsmeyer−Peppas, and Hixson-Corwell are clearly described in the equations (S10)-(S14).

$$Q_t = Q_o + k_o t \quad \text{(S10)}$$

$$\log Q_t = \log Q_o - k_1 t \quad \text{(S11)}$$

$$Q_t = k_H t^{1/2} \quad \text{(S12)}$$

$$Q_t / Q_\infty = k_{KP} t^n \quad \text{(S13)}$$

$$W_o^{1/3} - W_t^{1/3} = k_{HC} t \quad \text{(S14)}$$

Where Q_o, Q_t, and Q_∞ are the original amount of Cur, cumulative Cur release at *t* time, and at infinite time, respectively. n is the release exponent of the Korsmeyer−Peppas model. W_o and W_t are the cubic root of the Cur remaining content at original and *t* time, respectively. k_o, k_1, k_H, k_{KP}, and k_{HC} are the rate constants of the zero-order, first-order, Higuchi, Korsmeyer−Peppas, and Hixson-Corwell models.

Table S1. The data calculated from the isothermal models for the Cur loading onto ZIF-68

Isotherms	**Paramaters**	**Value**
Langmuir	q_m (mg g^{-1})	**833.3**
	K_L (L mg^{-1})	0.013
	R^2	**0.996**
	R_L	0.1
Freundlich	1/n	0.5381
	K_F (mg g^{-1} (L $g^{-1})^{1/n}$)	33.61
	R^2	**0.960**
Temkin	b	13.48
	k_T (L mg^{-1})	0.094
	R^2	**0.982**
Dubinin-Radushkevich (DR)	C (mol^2 J^2)	3.9×10^{-5}
	k_{DR} (mg g^{-1})	537.32
	R^2	**0.769**

Table S2. Pseudo-first-order and second-order-models parameters for the adsorption of Cur over ZIF-68

Kinetic models	**Paramaters**	**Value**
Pseudo-first-order	q_e (mg g^{-1})	**16.68**
	K_f (min^{-1})	0.0175
	R^2	**0.986**
Pseudo-second -order	q_e (mg g^{-1})	**19.16**
	k_s (10^{-3}) (g mg^{-1} min^{-1})	1.444
	R^2	**0.999**

Table S3. The maximum uptake capacities of Cur onto the various reported carriers

Materials	**Maximum uptake capacity ($mg\ g^{-1}$)**	**Ref.**
Ca-BDC	140.0	[1]
CD-MOF	150.0	[2]
Zein/SACD nanofibers	35.7	[3]
ZIF-8@BPMO	666.0	[4]
UiO-66-NH_2	180.0	[5]
Fe-MOF	145.6	[5]
Zn-BDC-NH_2	179.4	[6]
Zr-UiO-66	466.4	[7]
Zr-UiO-66-NH_2	382.9	[8]
APTES-CMF/ZIF-8	626.4	[9]
ZIF-68	**720.1**	**This study**

Table S4. Cytotoxicity of ZIF-68, and Cur@ZIF-68 in HDF cells and MCF-7 cells

Materials	**Concentration ($\mu g\ mL^{-1}$)**	**Cytotoxicity with HDF cell (%)**	**Cytotoxicity with MCF-7 cell (%)**
ZIF-68	5	82.4	90.0
	10	74.5	85.9
	15	67.6	74.1
	20	62.2	65.2
	25	56.8	48.1
Cur@ZIF-68	5	93.4	80.3
	10	85.5	70.6
	15	82.7	65.2
	20	80.0	47.5
	25	**74.2**	**28.1**

References

[1] George, P., Das, R. K., & Chowdhury, P., Facile microwave synthesis of Ca-BDC metal organic framework for adsorption and controlled release of Curcumin, *Microporous and Mesoporous Materials*, 2019, **281**, 161-171.

[2] Su, Q., Liang, M., Xing, S., & Tan, M., Multi-sites interactions of turmeric-derived curcumin in cyclodextrin metal-organic framework for the enhanced adsorption and solubility in apple juice, *Food Hydrocolloids*, 2025, **170**, 111747.

[3] Hu, Y., Rees, N. H., Qiu, C., Wang, J., Jin, Z., Wang, R., Zhu, Y., Chen, H., Wang P., Liu, S., Ren, F. & Williams, G. R., Fabrication of zein/modified cyclodextrin nanofibers for the stability enhancement and delivery of curcumin, *Food Hydrocolloids*, 2024, **156**, 110262.

[4] Nguyen, T. T. T., Le, B. Q. G., Dang, M. H. D., Phan, B. T., Mai, N. X. D., & Doan, T. L. H., Facile synthesis of novel fluorescent organosilica-coated MOF nanoparticles for fast curcumin adsorption, *Microporous and Mesoporous Materials*, 2022, **338**, 111944.

[5] El-Shafey, A. A., Hegab, M. H., Seliem, M. M., Barakat, A. M., Mostafa, N. E., Abdel-Maksoud, H. A., & Abdelhameed, R. M., Curcumin@metal organic frameworks nano-composite for treatment of chronic toxoplasmosis, *Journal of materials science: Materials in Medicine*, 2020, **31**, 90.

[6] Dang, Y. T., Dang, M. H. D., Mai, N. X. D., Nguyen, L. H. T., Phan, T. B., Le, H. V., & Doan, T. L. H., Room temperature synthesis of biocompatible nano Zn-MOF for the rapid and selective adsorption of curcumin. Journal of Science: Advanced Materials and Devices, 2020, **5**, 560-565.

[7] Dang, Y. T., Hoang, H. T., Dong, H. C., Bui, K. B. T., Nguyen, L. H. T., Phan, T. B., Kawazoe, Y. & Doan, T. L. H., Microwave-assisted synthesis of nano Hf-and Zr-based metal-organic frameworks for enhancement of curcumin adsorption, *Microporous and Mesoporous Materials*, 2020, **298**, 110064.

[8] Molavi, H., Zamani, M., Aghajanzadeh, M., Kheiri Manjili, H., Danafar, H., & Shojaei, A., Evaluation of UiO-66 metal organic framework as an effective sorbent for Curcumin's overdose, *Applied Organometallic Chemistry*, 2018, **32**, e4221.

[9] Wijanarko, M. G., Widagdo, A. J., Ismadji, M. S., Kusuma, K., Yuliana, M., Ismadji, S., Hartono, S. B., Lie, J., Shu, H., Abdullah, H., Kadja, G. T. M., Wijaya, C. J. & Soetaredjo, F. E., Utilization of APTES-functionalized coconut waste-based cellulose microfiber/zeolitic-imidazolate framework-8 composite for curcumin delivery, *Materials Today Sustainability*, 2023, **21**, 100332.